MOLECULAR IMAGING AND BIOLOGY

Published Online: 16 June 2010
Mol Imaging Biol (2011) 13:321–331
DOI: 10.1007/s11307-010-0368-z

RESEARCH ARTICLE

Increase of [^{18}F]FLT Tumor Uptake *In Vivo* Mediated by FdUrd: Toward Improving Cell Proliferation Positron Emission Tomography

David Viertl,[1] Angelika Bischof Delaloye,[1] Bernard Lanz,[2] Carole Poitry-Yamate,[2] Rolf Gruetter,[2] Vladimir Mlynarik,[2] Simon M. Ametamey,[3] Tobias L. Ross,[3] Hans-Anton Lehr,[4] Pierre-Alain André,[1] Florence Perillo-Adamer,[5] Marek Kosinski,[1] Yves M. Dupertuis,[6] Franz Buchegger,[1,7]

[1]*Service of Nuclear Medicine, University Hospital of Lausanne, CH-1011 Lausanne, Switzerland*
[2]*Laboratory for Functional and Metabolic Imaging, Swiss Federal Institute of Technology of Lausanne, CH-1015 Lausanne, Switzerland*
[3]*Center for Radiopharmaceutical Science, Swiss Federal Institute of Technology of Zurich, CH-8093 Zürich, Switzerland*
[4]*Institute of Pathology, University Hospital of Lausanne, CH-1011 Lausanne, Switzerland*
[5]*Service of Radio-Oncology, University Hospital of Lausanne, CH-1011 Lausanne, Switzerland*
[6]*Service of Nutrition, University Hospital of Geneva, CH-1211 Geneva, Switzerland*
[7]*Service of Nuclear Medicine, University Hospital of Geneva, CH-1211 Geneva, Switzerland*

Abstract

Purpose: 3′-deoxy-3′-[^{18}F]fluorothymidine ([^{18}F]FLT), a cell proliferation positron emission tomography (PET) tracer, has been shown in numerous tumors to be more specific than 2-deoxy-2-[^{18}F]fluoro-D-glucose ([^{18}F]FDG) but less sensitive. We studied the capacity of a nontoxic concentration of 5-fluoro-2′-deoxyuridine (FdUrd), a thymidine synthesis inhibitor, to increase uptake of [^{18}F]FLT in tumor xenografts.

Methods: The duration of the FdUrd effect *in vivo* on tumor cell cycling and thymidine analogue uptake was studied by varying FdUrd pretreatment timing and holding constant the timing of subsequent flow cytometry and 5-[^{125}I]iodo-2′-deoxyuridine biodistribution measurements. In [^{18}F]FLT studies, FdUrd pretreatment was generally performed 1 h before radiotracer injection. [^{18}F]FLT biodistributions were measured 1 to 3 h after radiotracer injection of mice grafted with five different human tumors and pretreated or not with FdUrd and compared with [^{18}F]FDG tumor uptake. Using microPET, the dynamic distribution of [^{18}F]FLT was followed for 1.5 h in FdUrd pretreated mice. High-field T2-weighted magnetic resonance imaging (MRI) and histology were used comparatively in assessing tumor viability and proliferation.

Results: FdUrd induced an immediate increase in tumor uptake of 5-[^{125}I]iodo-2′-deoxyuridine, that vanished after 6 h, as also confirmed by flow cytometry. Biodistribution measurements showed that FdUrd pretreatment increased [^{18}F]FLT uptake in all tumors by factors of 3.2 to 7.8 compared with controls, while [^{18}F]FDG tumor uptake was about fourfold and sixfold lower in breast cancers and lymphoma. Dynamic PET in FdUrd pretreated mice showed that [^{18}F]FLT uptake in all tumors increased steadily up to 1.5 h. MRI showed a well-vascularized homogenous lymphoma with high [^{18}F]FLT uptake, while in breast cancer, a central necrosis shown by MRI was inactive in PET, consistent with the histomorphological analysis.

Correspondence to: David Viertl; *e-mail:* David.Viertl@chuv.ch

Conclusion: We showed a reliable and significant uptake increase of [18F]FLT in different tumor xenografts after low-dose FdUrd pretreatment. These results show promise for a clinical application of FdUrd aimed at increasing the sensitivity of [18F]FLT PET.

Key words: [18F]FLT, PET, FdUrd, Thymidine synthesis, Cell proliferation

Introduction

Positron emission tomography (PET) is routinely used for cancer diagnosis, staging, and therapy monitoring. In many cancers, tumor cell proliferation is an important prognostic factor and is a key factor to monitoring efficacy of anticancer therapy. Therefore, radiopharmaceuticals directly related to cell proliferation, such as 3′-deoxy-3′-[18F]fluorothymidine ([18F]FLT), which targets the DNA synthesis, are highly relevant, and are promising for PET applications.

Several reagents have been proposed for PET imaging or γ-scintigraphy of tumor cell proliferation, including [123I] and [124I]iodo-2′-deoxyuridine (IdUrd,), [76Br]bromodeoyxuridine, [11C]thymidine, and derivatives of deoxy-[18F]fluoro-arabinofuranosyl such as [18F]FAU, [18F]FMAU, [18F]FBAU, and [18F]FIAU. While a number of these radiotracers were tested in clinical studies, [18F]FLT has emerged as the most promising PET tracer in recent studies [1]. Currently, several prospective clinical trials involving [18F]FLT are ongoing in patients with breast, lung, head, and neck cancer and glioblastoma (NCT00566293, NCT01015131, NCT00534274, NCT00847509, NCT00721799, NCT00624728).

[18F]FLT has several advantages compared with some of the other radiopharmaceuticals. While [11C]thymidine or radio-IdUrd derivatives are rapidly degraded *in vivo*, [18F]FLT is biologically stable and crosses the cell membrane by specific nucleoside transporters. Once in the cytoplasm, [18F]FLT is trapped through phosphorylation by thymidine kinase 1. Since thymidine kinase 1 expression increases in cells undergoing DNA synthesis (S phase), cytoplasmic uptake of [18F]FLT reflects the proliferative activity of cells [2]. Prior studies have established that [18F]FLT uptake correlates with Ki-67 immunostaining proliferation assay, in breast cancer [3], lung cancer [4], and leukemia [5], and with S phase fraction in lung tumors as measured by flow cytometry [6]. Tumor imaging with [18F]FLT PET has been shown to be generally specific in cancer diagnosis [7]. However, nonspecific incorporation can be observed in proliferating macrophages in inflammatory lesions [8]. It also appears to predict outcome after chemotherapy [9], radiotherapy [10] as well as progression and overall survival of patients with brain tumors [11]. Moreover, in breast cancer [12] and in high-grade non-Hodgkin's lymphoma [13], early change in [18F]FLT uptake, immediately after initiation of chemotherapy predicts tumor response to treatment. Thus, [18F]FLT might be an important adjunct in the therapeutic management of cancer patients.

Currently, 2-deoxy-2-[18F]fluoro-D-glucose ([18F]FDG) is the most frequently used PET imaging agent for characterization of mass lesions and assessment of response to treatment in a variety of tumors [14]. [18F]FDG, as a glucose analogue, is internalized in cells with enhanced glucose requirement. [18F]FDG incorporation has been found to be correlated with cellular proliferation [15] and, hence, has been considered an indicator of tumor aggressiveness [16]. However, it is a matter of debate whether glucose consumption is a good indicator of tumor aggressiveness. [18F]FDG uptake is not specific for tumor cells and can be found in nonneoplastic lesions, notably in inflammation and repair. Furthermore, high physiological cerebral glucose uptake limits its usefulness in brain tumor imaging.

Different studies have shown higher specificity of [18F]FLT in comparison with [18F]FDG [17], but lower sensitivity due to limited [18F]FLT tumor uptake. This is a major drawback for its widespread clinical application. In fact, only cells undergoing division are susceptible to incorporation of [18F]FLT. Moreover, injected [18F]FLT has to compete with endogenous thymidine, which further limits its uptake in proliferating cells.

In this study, we addressed part of these limitations by modifying cellular uptake of extracellular thymidine, by interfering with the endogenous DNA synthesis pathway using 5-fluoro-2′-deoxyuridine (FdUrd, floxuridine). We hypothesized that pretreatment with FdUrd might be able to increase tumor uptake of [18F]FLT. Here, FdUrd was used in mice at a nontoxic bolus injection of 2.5 mg/kg, while intravenous (i.v.) bolus treatment in humans is performed with 30 mg/kg [18]. We studied the effect of FdUrd in mice bearing different human tumor xenografts by biodistribution studies and animal PET.

Materials and Methods

Radiopharmaceuticals and Reagents

[18F]FLT was produced at the Center for Radiopharmaceutical Science of the Swiss Federal Institute of Technology at Zürich (Switzerland) according the procedure reported by Kim et al. [19]. The specific activity was 281±204 GBq/μmol, and the purity was ≥97% for all preparations.

5-[125I]iodo-2′-deoxyuridine ([125I]IdUrd) of high radiochemical purity was prepared in house using a modified method, originally described by Foulon et al. [20]. In all experiments, [125I]IdUrd represented ≥97% of overall I-125 activity.

Clinical grade [^{18}F]FDG was provided by Advanced Accelerator Applications (AAA; Saint Genis Pouilly, France).

FdUrd and 5′-deoxythymidine (dThd) were obtained from Sigma-Aldrich Chemie GmbH (Steinheim, Germany). IdUrd (Sigma-Aldrich Chemie GmbH) was dissolved in distilled water using NaOH alkalinization at minimally required concentration.

Cell Lines and Culture

Two Burkitt lymphomas (Ramos and BL60.2), two human breast adenocarcinomas (MDA-MB231, SKBR127), and two human colon adenocarcinomas (WiDr, LS174T9) were used. All cell lines except BL60.2 (kindly provided by Dr. Stephan Mathas at Delbrück-Center for Molecular Medicine, Berlin, Germany) were obtained from American Type Culture Collection. Cells were cultured at 37°C and 5% CO_2 in RPMI 1640 containing glutamax I (Invitrogen, Grand Island, NY) supplemented with 10% heat-inactivated fetal bovine serum (Chemie Brunschwig AG, Basel, Switzerland), penicillin (50 units/mL) and streptomycin (0.05 mg/mL; from Life Technologies Inc., Grand Island, NY).

Since mycoplasma contamination is a source of increased nucleoside turnover that therefore modulates FdUrd efficacy and cellular uptake of thymidine, cells were cultured for 6 months after thawing and tested negative for mycoplasma contaminations (Mycoplasma Detection Kit; F. Hoffmann-La Roche Ltd, Basel, Switzerland).

Mice and Tumor Models

All experiments were performed according to the principles of laboratory animal care and Swiss legislation. The experiments were specifically approved by the official committee on surveillance of animal experiments. Female homozygous athymic Foxn1$^{nu/nu}$ nude and CB17 SCID mice were obtained from Harlan Laboratories (Boxmeer, Netherlands). Animals were kept under specific pathogen-free conditions, in autoclaved filter-topped cages and bedding in a separate room. Mice had access *ad libitum* to sterilized food and water.

Suspensions of 5×10^6 cells in 0.07 to 0.1 mL cell culture media were inoculated subcutaneously at inguinal (for biodistribution studies) or thoracic level (for PET studies) in mice of 6 to 8 weeks of age. Experiments were performed after adequate growth of tumors 12 days to 4 weeks after grafting. For experiments including magnetic resonance imaging (MRI), tumors were grafted subcutaneously onto the skull of mice.

Flow Cytometry and [^{125}I]IdUrd Incorporation Measurements

For these experiments, pretreatment timing was varied between FdUrd injection and IdUrd or [^{125}I]IdUrd injection. The timing of analysis post-IdUrd injection was 1 h after unlabeled IdUrd and 5 h after [^{125}I]IdUrd.

Tumor xenografts were analyzed by two-parameter flow cytometry. Mice bearing BL60.2 and Ramos tumors received 3, 10, or 30 mg/kg FdUrd i.v. After varying pretreatment intervals (1, 3, and 6 h), the animals were injected intraperitoneally with 1 mg IdUrd and euthanized by CO_2 inhalation 1 h thereafter. Control groups were not pretreated with FdUrd and received only IdUrd. Tumors were excised, dissociated with a tissue grinder, and washed. Aliquots of 10^6 cells were labeled with anti-BrdU fluorescein isothiocyanate (FITC) and propidium iodide following the method in the Becton Dickinson source book section 3.80.1 (Becton Dickinson Immunocytometry Systems, San Jose, CA). Flow cytometry (FACScan; Becton Dickinson, Franklin Lakes, NJ) was performed with a laser excitation at 488 nm for PI and FITC fluorescence.

Two days before [^{125}I]IdUrd biodistribution measurements, mice were given 0.2 g/L KI in drinking water to block I-125 uptake in thyroid and 1 g/L $KClO_4$, to inhibit iodine secretion in stomach. Mice were pretreated with 5 mg/kg FdUrd injected i.v. in 2 fractions separated by 30 min. After (1, 3, and 10 h) FdUrd pretreatment, 10 kBq [^{125}I]IdUrd was injected into tumor. Animals were euthanized 5 h after [^{125}I]IdUrd injection, and biodistribution was measured in dissected tumors and tissues. Mean ± 1 SD of results were expressed in percentage of injected dose per gram tissue (% ID/g).

[^{18}F]FLT and [^{18}F]FDG Biodistribution Studies

The effect of mild FdUrd conditioning on [^{18}F]FLT tumor uptake was assessed in mice bearing Ramos, MDA-MB231, SKBR3, LS174T, and WiDr xenografts. The protocol used for biodistribution studies was adapted from Dupertuis et al. [21].

FdUrd pretreated mice received a single i.v. injection of 2.5 mg/kg FdUrd, and 1 h after FdUrd injection, unless stated differently, 1 MBq [^{18}F]FLT was injected in the lateral tail vein. In one experiment, a 10-min delay after FdUrd was compared with a 1-h delay. Control mice received [^{18}F]FLT only. Mice were euthanized by CO_2 inhalation, 1, 2, or 3 h after [^{18}F]FLT administration. The tumors, all major normal organs (liver, kidney, lung, spleen, heart, stomach, and large and small intestine) and samples of tissues (blood, quadriceps muscle, skin, and femoral bone) and the rest of the carcasses were dissected and weighted, and radioactivity was measured in a γ-counter (1480 Wizard 3; PerkinElmer, Schwerzenbach, Switzerland).

Specificity of [^{18}F]FLT tissue uptake under FdUrd enhancement was assessed by competition experiments, using an excess of dThd. Both injections of FdUrd and [^{18}F]FLT were enriched with 20 mg/kg dThd each.

Biodistributions of [^{18}F]FDG were measured in groups of four mice bearing both MDA-MB231 and SKBR3 tumors and five mice with double grafts of Ramos tumors. Mice were fasted for a minimum of 6 h before i.v. injection of 1 MBq [^{18}F]FDG. During [^{18}F]FDG experiments, mice were maintained under anesthesia using 1% isoflurane delivered in oxygen at 1 L/min and warmed to 31°C. Two hours after [^{18}F]FDG administration, mice were euthanized by CO_2 inhalation and dissected, and organs were weighed and counted as previously described.

Small-Animal PET

Imaging was performed using an avalanche photodiode microPET scanner (LabPET4; Gamma Medic-Ideas, Sherbrooke, Quebec, Canada). During the entire scanning period, mice were maintained under 1% isoflurane anesthesia in oxygen delivered at 1 L/min using a face mask and under monitoring of temperature and breathing rate. For dynamic PET, all animals were pretreated with 2.5 mg/kg FdUrd. List-mode acquisitions of 90 min were initiated 1 min after injection of 24.8±6.0 MBq [^{18}F]FLT, via the lateral tail vein. An energy window of 250–650 keV and a coincidence-timing

window of 22.2 ns were used. Images were reconstructed by the MLEM iterative method. Images were corrected for nonuniformity of scanner response, dead time count losses, and physical decay to the time of injection.

Images were analyzed with the PMOD 3.0 software (PMOD Technologies, Zurich, Switzerland). For dynamic studies, regions of interest were drawn manually by optical reading of well-delineated normal tissues like heart on early frames and tumors on late frames. These regions of interest were then projected on all dynamic images. Time activity curves were calculated for different areas (tumor, heart, bone, and abdominal activity) and were expressed in kBq/mL.

Magnetic Resonance Imaging

Scans were performed on a 9.4 Tesla Varian (Varian Medical Systems, Palo Alto, CA) 21-cm horizontal-bore scanner with a 12-cm 200-mT/m gradient insert (Magnex Scientific, Oxford, UK) [22]. Respiration was monitored during the measurement, and body temperature was maintained at 37°C. MRI was performed for head implanted tumors, using tight immobilization of the animal head with bilateral ear pins and maxillary fixation. Multislice fast-spin-echo T2-weighted images (using a repetition time of 4 s and an echo time of 50 ms) were obtained in the coronal and transverse planes using a field of view of 20×20 mm, a slice thickness of 0.7 mm, and a matrix size of 256×256 image voxels.

Tumor Histology and Immunohistochemistry

Tumors were fixed with 4% neutral buffered formalin and embedded in paraffin. For Ki-67 immunostaining, 4-μm-thick sections were cut from paraffin blocks, deparaffinized in xylene, and rehydrated in graded ethanol. Sections were incubated overnight at 4°C with monoclonal mouse antihuman Ki-67 antibody (Dako Schweiz, Baar, Switzerland). For determination of tumor proliferative rate, 1,000 cells per slide were counted at 40× magnification using a standard diagnostic microscope and KI-67-positive cells expressed in percentage of total tumor cells. Standard hematoxylin–eosin (HE) staining was used for evaluation of tumor cell viability and general histological examination. The mitotic index of each tumor was determined by counting the number of mitotic figures on 10 different 40× magnification field of views. Data were expressed as mean ± 1 SD per 10 high power field (HPF).

Statistical Analysis

To evaluate the increase in the mean tumor uptake values during the late period (20 last min) of dynamic PET scanning, two different time frames were compared with each other using the Student's *t* test. The activity measured over five frames of 1 min each, one starting at 66 min, and the other at 86 min was compared, and P values < 0.05 were considered statistically significant. The Mann–Whitney nonparametric test was used to assess whether tumor uptake of [^{18}F]FLT in FdUrd-pretreated animals was different from control groups, $P<0.05$ being considered significant and $P<0.01$ highly significant. Both statistical tests were two sided. Tests were performed using the statistical analysis software SPSS (version 15.0; SPSS, Inc., Chicago, IL).

Results

Timing Dependence of FdUrd Efficacy on Tumor Cells In Vivo

Cell cycle modification induced by FdUrd *in vivo* was studied by flow cytometry experiments. In BL60.2 and Ramos lymphoma tumors, cell cycle determination was only possible in mice having been pretreated with FdUrd. Without FdUrd pretreatment, IdUrd based S phase staining failed to produce a measurable two-dimensional separation of cells. In BL60.2 cells, the ratio of S phase cells was already high at 1 h after administration of FdUrd (50.6%±7.3%) and was similar at 3 h (50.4%±2.7%). Thereafter, the staining of S phase cells was lost and no longer measurable at 6 h after FdUrd pretreatment. Similarly, in mice bearing Ramos tumors, the number of cells in S phase was very high (61.7%±0.2% of the whole viable cell population) but limited in time, and at 6 h post-FdUrd, the signal vanished (Fig. 1; Table 1). Variations in the amount of FdUrd injected (3, 10, and 30 mg/kg) did not

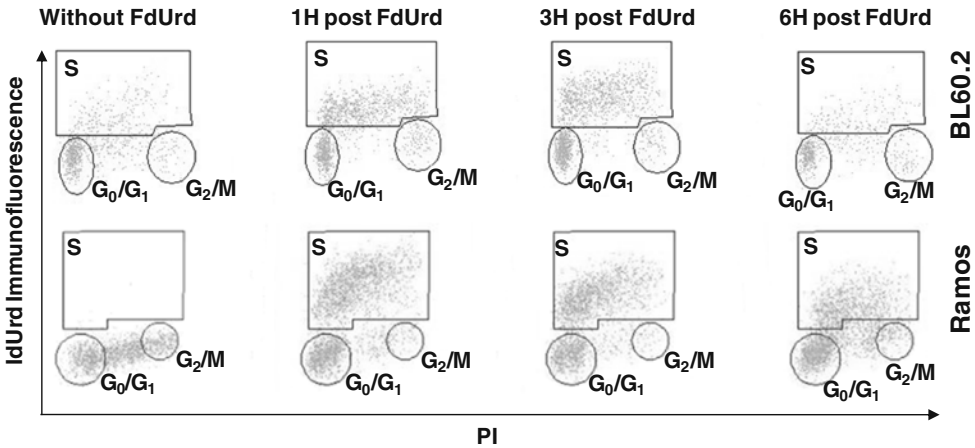

Fig. 1. Examples of flow cytometry histograms of cell distribution in the cell cycle stages (G_0/G_1, S, and G_2/M). Results without FdUrd pretreatment or at 1, 3, and 6 h post-30 mg/kg FdUrd i.v. injection are shown.

Table 1. Percentage of cells in the G0/G1, S, and G2/M phase of the cell cycle as observed by double-staining flow cytometry

		Without FdUrd	1 h post-FdUrd	3 h post-FdUrd	6 h post-FdUrd
BL60.2	G_1/G_0	N.A[a]	34%±3%	36%±3%	44%±2%[b]
	S	NA[a]	51%±7%	50%±3%	24%±7%[b]
	G_2/M	NA[a]	7%±1%	5%±1%	8%±1%[b]
Ramos	G_1/G_0	NA[a]	35%±1%	30%±1%	44%±2%[b]
	S	NA[a]	56%±1%	62%±1%	34%±1%[b]
	G_2/M	NA[a]	2%±1%	2%±1%	6%±1%[b]

[a]Nonapplicable or [b]partially relevant only in the case of two-parameter flow cytometry due to insufficient incorporation of exogenous IdUrd

provide differences in the percentage of cells in S phase nor in the duration of measurable S phase staining (results not shown).

The effect of FdUrd over time was also assessed by biodistribution measurements of [125I]IdUrd in mice bearing Ramos tumors. Three pretreatment time points (1, 3, and 10 h) between FdUrd and intratumoral injection of [125I]IdUrd were chosen. Mice were euthanized 5 h after [125I]IdUrd injection, and the residual activity found in tumor and normal tissues was counted. The baseline activity without FdUrd pretreatment was 29.5%±8.5% ID/g in the tumors. With 1 h between FdUrd and [125I]IdUrd injections, tumor activity was significantly increased to a peak of 256.2%±81.9% ID/g. As the interval between FdUrd and [125I]IdUrd injections increased, the intratumoral activity decreased to 99.6%±5.0% and 56.3%±1.3% ID/g at 3 and 10 h, respectively.

[18F]FLT and [18F]FDG Biodistribution Studies

The effect of a single injection of 2.5 mg/kg FdUrd i.v. 1 h before injection of [18F]FLT was tested in mice grafted with different types of human tumors.

In four groups of mice bearing Ramos lymphoma xenografts, biodistribution of [18F]FLT was measured at 1 and 3 h after injection of [18F]FLT. Tumor uptake of [18F]FLT in control mice (without FdUrd pretreatment) was moderate with 7.7%±1.3% and 9.4%±1.5% ID/g at 1 and 3 h, respectively. In FdUrd-pretreated mice, [18F]FLT tumor uptake was significantly increased with 42.4%±5.8% and 41.3%±5.8% ID/g at 1 and 3 h, respectively (Fig. 2a; Table 2). Due to washout from nonneoplatsic tissues, high retention of [18F]FLT in tumors of pretreated mice led to markedly improved tumor-to-normal-tissue ratios at 3 h after [18F]FLT injection (Fig 2b). The absence of increased [18F]FLT uptake in spleen and bone marrow after FdUrd pretreatment in these mice might be explained by the fact that they had been treated by whole-body irradiation (2.5 Gy) before tumor transplantation in order to facilitate engraftment of the lymphoma. The biodistribution experiment was performed 11 days after irradiation when bone marrow and spleen cells remained depressed. Biodistribution of [18F]FDG in fasted and anesthetized mice showed that the Ramos tumors incorporated 6.7%±1.2% ID/g 2 h after [18F]FDG injection (Fig. 2c).

Based on the results in lymphoma xenografts and clinical experience reporting a higher sensitivity by increasing the delay between injection and acquisition in [18F]FDG PET in breast cancer, biodistribution of [18F]FLT in mice grafted with MDA-MB231 and SKBR3 human breast carcinomas was measured 2 h after injection of [18F]FLT. FdUrd enhanced the uptake of [18F]FLT in MDA-MB231 and SKBR3, compared with nonpretreated mice, by a mean factor of 4.7 and 3.2, respectively (Fig. 3a; Table 2). In MDA-MB231 tumors, baseline incorporation of [18F]FLT was 6.3%±1.6% ID/g rising, after FdUrd pretreatment, to 29.4%±5.8% ID/g. In SKBR3 tumors, uptake in untreated mice was 5.3%±1.0% ID/g compared with 17.1%±4.7% ID/g after FdUrd injection (Fig. 3a; Table 2).

The specificity of the [18F]FLT uptake in FdUrd pretreated mice was confirmed by competitive inhibition with an excess of dThd. In these mice, tumor uptake decreased to 2.0%±0.5% and to 2.4%±0.6% ID/g in MDA-MB231 and SKBR3 xenografts, respectively (Fig. 2a).

For comparison, [18F]FDG biodistribution was performed 2 h postinjection in fasted and anesthetized mice bearing also MDA-MB231 and SKBR3 breast cancer xenografts. The [18F]FDG tumor uptake was 6.6%±0.4% and 4.3%±1.0% ID/g in MDA-MB231 and SKBR3 tumors, respectively (Fig. 3b). We had obtained very similar [18F]FDG biodistribution and tumor uptake results, except for muscle, in a pilot study in nonanesthetized, but otherwise identically treated mice (results not shown).

In a separate experiment aiming to further optimize the accumulation of [18F]FLT within tumor cells, the timing of injection was varied in groups of three mice, each bearing two xenografts of the MDA-MB231 breast cancer cell line. In mice without FdUrd pretreatment, the baseline tumor incorporation of [18F]FLT, measured 2 h after radiotracer injection, was rather low with 2.1%±0.2% ID/g. FdUrd pretreatment of mice 10 or 60 min before [18F]FLT injection and dissection at 2 h after radiotracer administration yielded a dramatic increase in tumor uptake, with mean values of 16.6%±2.1% and 15.8%±2.5% ID/g, respectively (Table 3). When mice, pretreated 1 h before injection of [18F]FLT, were analyzed at 1 h after radiotracer injection, tumor uptake of 15.8%±3.5% ID/g was very similar to the results of dissection after 2 h, but as expected, the activity in normal tissues was markedly higher at 1 h.

In order to reproduce these findings in another tumor type, the effect of FdUrd was measured in mice bearing LS174T and WiDr colon cancer xenografts. In control mice,

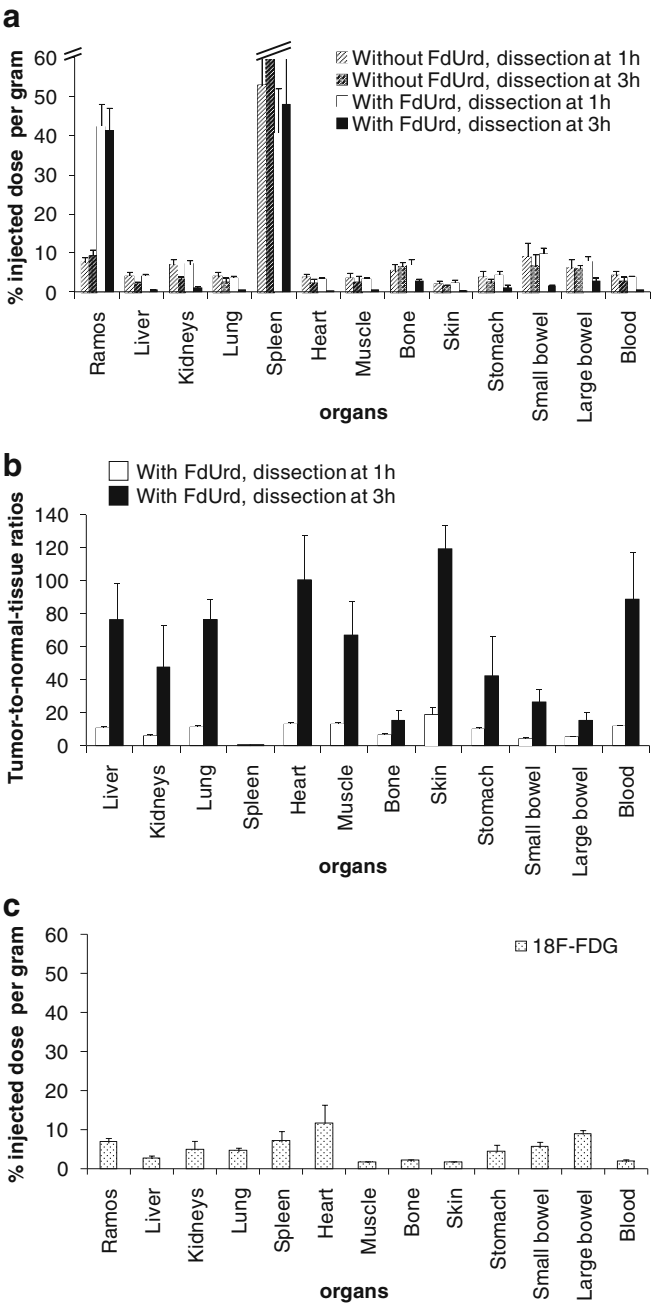

Fig. 2. **a** Biodistributions measured in mice bearing Ramos xenografts and euthanized 1 and 3 h, respectively, after i.v. injection of 1 MBq [18F]FLT. Column break (=): spleen = 80.9%±38.6% ID/g. **b** Histogram of the tumor-to-normal-tissue ratios in FdUrd-pretreated mice, in comparison with mice analyzed 1 and 3 h after [18F]FLT injection. **c** Biodistributions of [18F]FDG (*y*-scale same as in **a** to facilitate comparison).

tumor uptake was 8.5%±4.1% and 5.7%±2.2% ID/g in LS174T and WiDr, respectively. After FdUrd pretreatment, mean tumor uptake in LS174T and WiDr xenografts increased 4.3- and 5.8-fold, reaching 36.3%±14.5% and 32.9%±9.8% ID/g, respectively (Fig. 4; Table 2).

Table 2. Summary of the mean tumor uptake in control and FdUrd pretreated mice

Cell lines	T[a]	[18F]FLT tumor uptake (% ID/g)		Mean fold increase in uptake	Nb[b]
		Control	With FdUrd		
Ramos	1 h	7.7 ± 1.3	42.4±5.8**	5.5	4
	3 h	9.4±1.5	41.3±5.7**	4.4	3
MDA-MB231	2 h	6.3±1.6	29.4±5.8*	4.7	5
SKBR3	2 h	5.3±1.0	17.1±4.7*	3.2	5
LS 174T	2 h	8.5±4.1	36.3±14.5*	4.3	3
WiDr	2 h	5.7±2.2	32.9±9.8*	5.8	3

[a]Length of time between [18F]FLT injection and biodistribution measurement
[b]Number of mice per group
Mann–Whitney test *significantly different ($P<0.05$) and **highly different ($P < 0.01$)
Summary of the [18F]FLT tumor uptake with and without FdUrd pretreatment, for all the xenografts tested. Pretreatment of mice consisted of i.v. injection of 2.5 mg/kg FdUrd, 1 h before injection of 1 MBq [18F]FLT also i.v. The mice were euthanized 1, 2, or 3 h after [18F]FLT injection such as stated and biodistribution measured after dissection as described

Dynamic [18F]FLT PET

All tested tumors (Ramos, MDA-MB231, SKBR3, LS174T, and WiDr) continuously took up [18F]FLT over 90 min of dynamic PET (Fig. 5). For all tumors, the [18F]FLT activity was below intra-abdominal background activity immediately

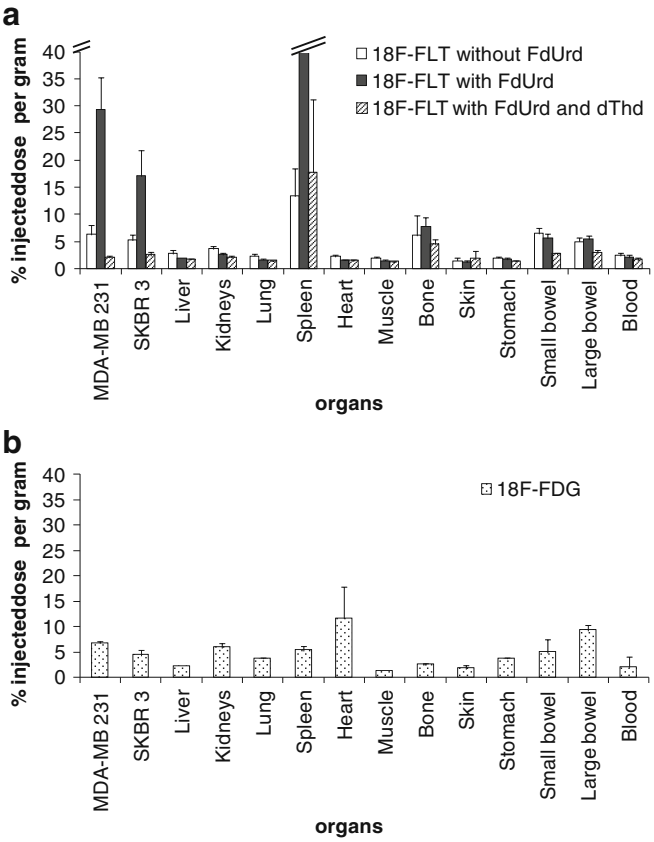

Fig. 3. **a** Biodistributions of [18F]FLT without or with FdUrd pretreatment in mice bearing MDA-MB231 and SKBR3 tumors. Column break (=): spleen = 79.3%±31.7% ID/g in mice with FdUrd pretreatment. **b** Biodistributions of [18F]FDG.

Table 3. [18F]FLT tumor and normal tissue uptake according to various timings for FdUrd pretreatment and euthanization of animals

	[18F]FLT uptake (% ID/g)			
Lapse of time between [18F]FLT injection and dissection	2 h			1 h
Lapse of time between FdUrd pretreatment and [18F]FLT injection	Control	1 h	10 min	1 h
MDA-MB231 tumor	2.1±0.2	15.8±2.5	16.6±2.1	15.8±3.5
Liver	0.8±0.1	1.0±0.3	0.8±0.1	2.1±0.1
Kidneys	1.1±0.2	1.3±0.2	1.2±0.1	2.6±0.1
Lung	0.1±0.1	0.7±0.1	0.8±0.1	1.8±0.1
Spleen	6.1±0.6	46.7±8.1	36.5±7.1	50.7±14.0
Heart	0.7±0.1	0.7±0.1	0.7±0.1	1.9±0.5
Muscle	0.6±0.1	1.4±1.4	0.7±0.0	1.5±0.2
Bone	5.1±1.4	8.4±2.4	9.6±1.0	12.6±3.4
Skin	0.5±0.2	0.5±0.0	0.4±0.1	1.5±0.2
Stomach	0.6±0.1	0.7±0.1	0.7±0.1	1.7±0.1
Small bowel	2.5±1.5	3.3±0.5	2.4±0.0	5.2±0.1
Large bowel	1.9±0.2	2.4±0.2	1.9±0.1	3.8±0.5
Blood	1.8±0.5	2.3±0.9	2.6±0.5	2.6±0.3

Mice with subcutaneous MDA-MB231 tumors (two tumors per animal) were not pretreated (controls) or pretreated with 2.5 mg/kg FdUrd in 0.2 mL saline i.v. After 10 or 60 min, 1-MBq [18F]FLT was also administered i.v. The animals were euthanized and organs dissected 1 or 2 h postradiotracer injection, and biodistribution was measured as described. Note the very similar tumor (and spleen) uptake at 1 and 2 h post-[18F]FLT injection. In contrast to tumor (and spleen), however, activity in the other normal tissues was significantly lower at 2 h compared with 1 h due to washout, leading to higher tumor-to-normal tissue ratios at 2 h

after injection. At 90 min, the activity accumulated within the tumors was higher than background by a magnitude ranging between factors of 2.7 (Ramos) and 7.5 (WiDr). Tumors continued to accumulate [18F]FLT during the last 20 min of dynamic PET imaging. The average activity increase per milliliter of tumor, between 68 and 88 min after [18F]FLT injection, ranged between 9.0% (Ramos) and 14.6% (WiDr; Table 4). In contrast, the background measured in abdomen steadily decreased over the time of observation in all mice. The activity in the heart, important within a few minutes after [18F]FLT injection, decreased rapidly to reach a level comparable with background.

Correlation of PET, MRI, and Histology of a Breast Cancer and Ramos Lymphoma

Imaging on animal-dedicated MRI and PET was performed at 1-day intervals in mice with MDA-MB231 breast cancer (Fig. 6) and Ramos tumor xenografts (Fig. 7). A macroscopic necrotic center of the MDA-MB231 appeared on MRI as a hyperintense structure surrounded by vital tumor. In contrast, the Ramos tumor appeared on MRI to be uniformly viable. The same tumors investigated by PET, using FdUrd pretreatment, showed that the entire Ramos tumor avidly incorporated [18F]FLT, whereas in MDA-MB231, a central hypoactive area in PET, corresponding to the necrotic portion in MRI, was surrounded by tumor accumulating [18F]FLT.

At the cellular level, histology showed that the Ramos tumor was close to 100% viable and showed a pronounced proliferative activity, as evidenced by immunohistochemistry. In different sections, the mitotic index was 87±22 mitoses /10 HPF, and virtually all tumor cells were MIB-1 positive. In the "viable" rim of MDA-MB231 tumor, 95% of cells were viable and the mitotic index was 37±14 mitoses/10 HPF, with a MIB-1 positivity rate of 70% to 80%. In the second breast cancer SKBR3, the "viable" tumor contained between 20% and 35% necrotic cells, while 58±26 mitoses/10 HPF were counted with a MIB-1 positivity rate of 90% to 95%.

Discussion

The tumor uptake of [18F]FLT has been shown in various clinical studies to be lower than with [18F]FDG [17, 23]. Despite the urgent need for a proliferation imaging agent, [18F]FLT PET remains confined to clinical studies in particular situations or as complement to [18F]FDG PET.

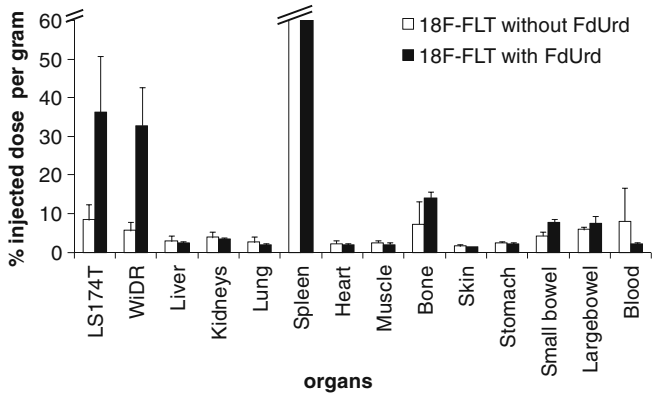

Fig. 4. Biodistributions of [18F]FLT in mice engrafted with LS174T and WiDr. Mice were not pretreated or pretreated with FdUrd 1 h before [18F]FLT injection. Results are expressed in percentage of injected dose per gram of tissue (mean ± 1 SD).Column break (=): spleen = 115.8%±116.6% and 102.6%±57.21% ID/g in mice without and with FdUrd pretreatment, respectively.

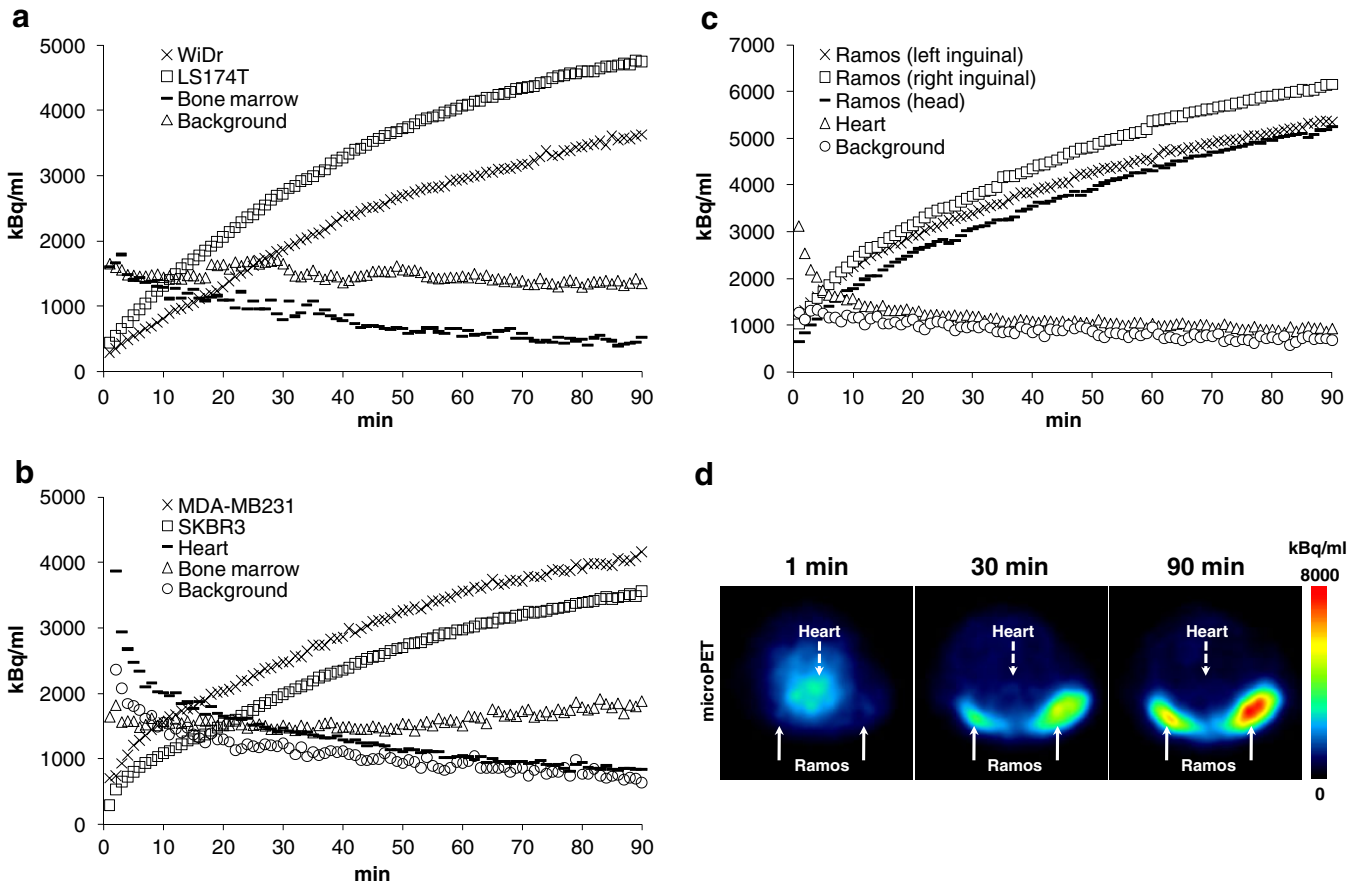

Fig. 5. Charts of dynamic PETs showing accumulation of [18F]FLT for 90 min in FdUrd pretreated mice: **a** WiDr and LS174T tumors. **b** MDA-MB231 and SKBR3 tumors. **c** Ramos lymphoma tumors. **d** PET images of [18F]FLT distribution in a mouse bearing the Ramos tumors.

Different groups have observed variable effects of [18F]FLT or [125I]IdUrd cellular uptake after exposure to therapeutic doses of chemotherapies such as 5-fluorouracil (5-FU) [24, 25] and others [26, 27] *in vitro* and in patients. These observations, considered as a "flare" phenomenon, were to be taken into account when interpreting [18F]FLT PET. In our approach, we used a single i.v. injection of a nontherapeutic dose of FdUrd, aimed at improving tumor uptake of [18F]FLT in order to use this procedure in diagnostic PET. We used a dosing and timing of FdUrd pretreatment that had been studied previously in experiments conducted with [125I]IdUrd [21] that is incorporated into DNA.

The endogenous thymidine pool competes with [18F]FLT uptake into proliferating cells. FdUrd directly blocks the endogenous thymidine synthesis without any major impact on other nucleotide pathways. The thymidine synthesis block enhances the salvage pathway and nucleoside transporters promoting enhanced cellular uptake of exogenous thymidine and thymidine analogs. As shown here, this strategy is well applicable to [18F]FLT PET. Since 5-FU is partially converted to FdUrd, this could explain the previously described enhanced uptake of [18F]FLT. Unfortunately, the conversion rate of 5-FU into FdUrd varies greatly among patients and adequate 5-FU dosing would be challenging. Furthermore, adverse effects due to the cytostatic action of 5-FU on RNA synthesis would limit its clinical usefulness in an imaging application [27].

Timing of PET after [18F]FLT injection has been variable in the literature. We therefore studied this aspect both with

Table 4. Increase of the [18F]FLT trapped in tumors during the last 20 min of dynamic PET shown in Fig. 5

	Average activity 66–70 min (kBq/mL)	Average activity 86–90 min (kBq/mL)	Percentage of increase
WiDr[a]	3,130±33*	3,586±31*	14.6
LS174T[a]	4,291±45	4,727±29	10.2
MDA-MB231[b]	3,702±30	4,071±54	9.9
SKBR3[b]	3,168±28	3,502±40	10.6
Ramos (left)[c]	4,841±44	5,338±25	10.3
Ramos (right)[c]	5,584±36	6,085±58	9.0
Ramos (head) [c]	4,200±39	4,654±28	10.8

[a]Tumors corresponding to Fig. 5a
[b]Tumors corresponding to Fig. 5b
[c]Tumors corresponding to Fig. 5c
*Activity of the [18F]FLT as measured in the different tumors (see Fig. 5) over 5 frames of 1 min each at 66 to 70 min and 86 to 90 min after injection is expressed as mean ± 1 SD. The measured uptake increase in percentage (last column) was significant for each tumor when comparing the five frames at around 68 min postinjection with those of 88 min

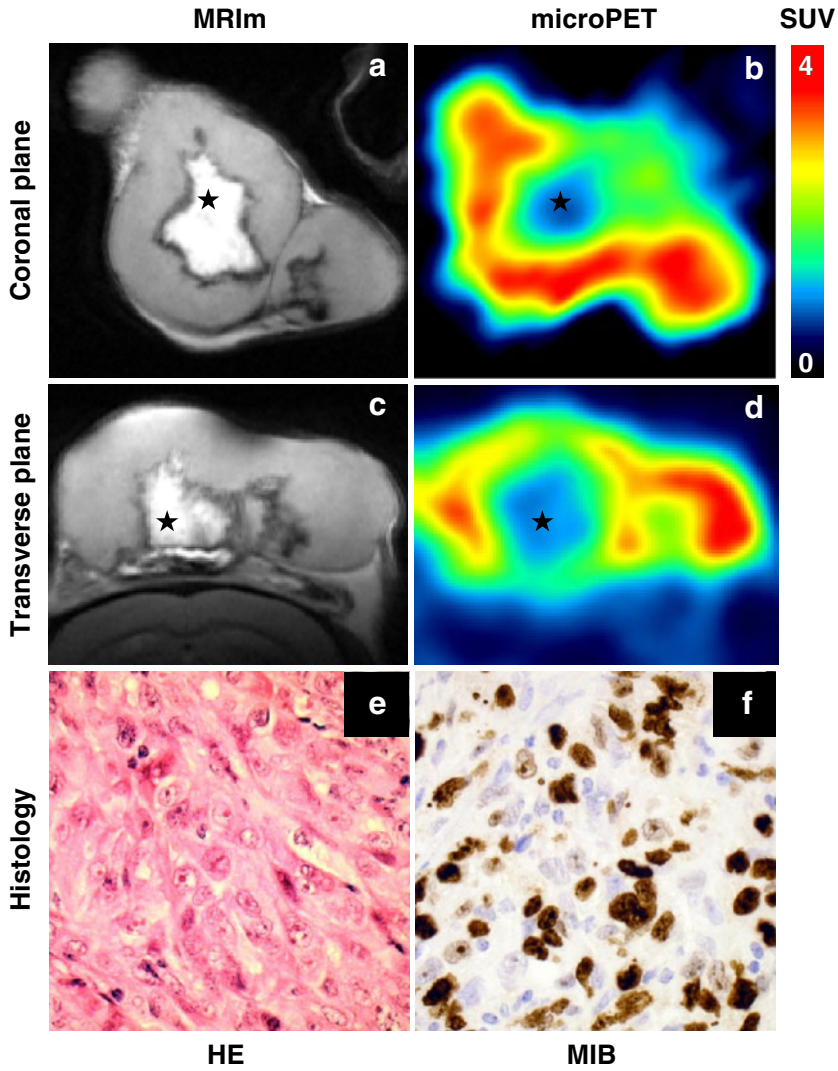

Fig. 6. MRI and PET of a MDA-MB231 tumor with a large central necrosis. T2-weighted images (**a, c**) obtained with MRI scanner. PET images (**b, d**) of the same animal were done 120 min after injection of [18F]FLT after FdUrd pretreatment. Note that the portion of tumor that incorporated the [18F]FLT corresponded to the viable tumor imaged by MRI. The *star* (★) shows the necrotic region of the tumor. A representative histological specimen of MDA-MB231 tumor was stained with HE (**e**) and MIB-1 (**f**). **e, f**: ×40 enlargement.

biodistribution experiments and a kinetic study with microPET. A timing experiment in lymphoma xenografts showed a very similar tumor uptake of [18F]FLT at 1 and 3 h after injection. In normal tissues, however, washout at 3 h was much higher than at 1 h, leading to improved tumor-to-normal tissue ratios.

The observation of prolonged retention of [18F]FLT in lymphoma prompted the evaluation of [18F]FLT for cell proliferation PET at 2 h after injection, which would be a compromise between the optimal tumor-to-normal tissue ratio observed at 3 h and the short physical half-live of F-18 of 110 min. Dynamic microPET imaging confirmed that tumor uptake increased up to 1.5 h after [18F]FLT injection in FdUrd pretreated mice. These results suggest that PET performed as early as 1 h after injection would not take optimal advantage of delayed uptake in the tumor cells and tracer elimination from normal tissues.

The results shown here with a low-dose FdUrd pretreatment of animals at 2.5 mg/kg may be clinically relevant as a diagnostic procedure. Indeed, in early patient treatment protocols, a bolus of FdUrd was injected daily i.v. at 30 mg/kg over the first 7 days, followed by further administrations of 15 mg/kg over several additional days [18]. Similarly, high doses of FdUrd have been used more recently for therapy with bolus injections of 3 g daily (~50 mg/kg) into the peritoneal cavity of patients with peritoneal tumor dissemination [28]. The difference between bolus injection and 24-h perfusion of FdUrd was studied by Sullivan et al. [29]. As compared with massive bolus treatments in patients, administration of a single dose of 2.5 mg/kg used here in mice is underdosed by a factor of 10 or more. Furthermore, in previous studies, we have also shown that a similar efficacy of FdUrd in mice was reached

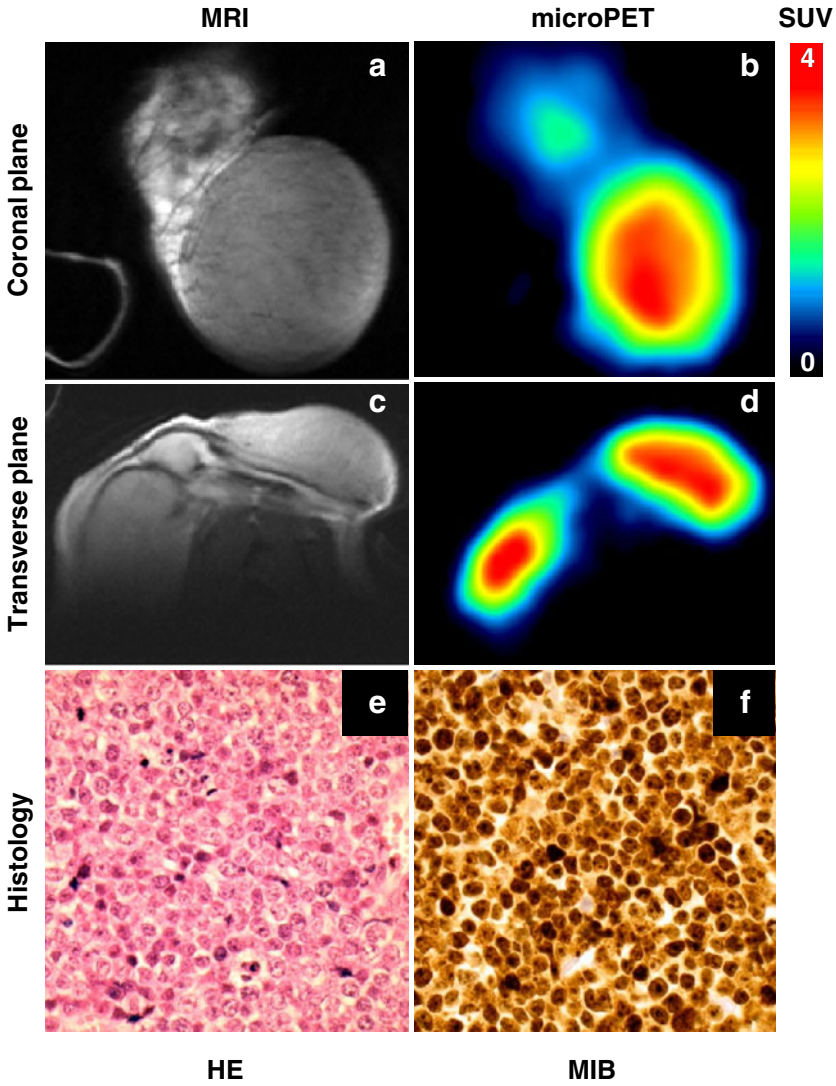

Fig. 7. MRI and PET of nonnecrotic Ramos tumor, obtained under the same conditions as Fig. 6. The MRI (**a, c**) and PET images (**b, d**) of the same tumors were acquired. Note that the whole tumor, which appears to be healthy by MRI, incorporated avidly [18F]FLT as revealed by PET. The Ramos tumor was subcutaneously grafted on the top of the head of a mouse. Representative histological specimen of the Ramos tumor, stained with HE (**e**) and MIB-1 (**f**). **e, f**: ×40.

with injections of between 1 and 3 mg/kg [21]. For a first clinical trial, we therefore propose the dose of 1 mg/kg FdUrd, corresponding to a 30- to 50-fold lower dose than reported in daily treatment protocols using bolus injections. While flow cytometry data from tumors grown *in vivo* suggested that FdUrd had a limited time of efficacy, in the range of about 6 h, this was also confirmed with incorporation studies with [125I]IdUrd. Finally, an innocuity test was performed in 10 mice given a single i.v. bolus injection of 100 mg/kg FdUrd. No adverse effect was observed in terms of body weight evolution over 2 months, leukocyte counts at 10 days after injection, nor organ appearance at macroscopic inspection at 60 days (results not shown). Based on these observations, we estimate that the clinical use of FdUrd at a dose of 1 mg/kg in a single bolus i.v. injection can be considered as safe and warrants a first clinical trial.

The competition from the endogenous thymidine pool for cellular uptake of exogenous [18F]FLT raises another interesting question pertaining to [18F]FLT PET. The endogenous thymidine pool and the efficacy of thymidine synthesis may vary from patient to patient and may likely fluctuate depending on the nutritional status. Such variations could lead to variable [18F]FLT tumor uptake even in cancers of similar proliferation activity. Hence, FdUrd could improve the consistency of [18F]FLT tumor uptake by uncoupling it from the endogenous thymidine pool. While serum glucose level is well monitored in patients undergoing [18F]FDG PET and subject to hormonal control, intracellular thymidine concentration cannot be measured before [18F]FLT PET. The potential of FdUrd to circumvent variations of the endogenous thymidine pool may thus present a major advantage for the clinical use of [18F]FLT PET.

In conclusion, our *in vivo* data showed a marked tumor uptake increase of [^{18}F]FLT in FdUrd pretreated mice that might be highly clinically relevant and warrants confirmation in patients. Such a study is being planned in patients with aggressive breast cancer. The information gained from the timing and biodistribution experiments has provided important clues for such a clinical trial. We thus propose performing PET imaging 2 h after [^{18}F]FLT injection, while pretreatment with FdUrd may be similarly efficient when administered between 10 to 60 min before injection of [^{18}F]FLT.

Acknowledgments. Major support of this work by the Swiss National Science Foundation Grant Nr3100AO-110023 is thankfully acknowledged. We express our gratitude to Mrs. Frances Godson for reviewing the manuscript. We also acknowledge the technical assistance of the laboratory of the Institute of Pathology at the University Hospital of Lausanne. We gratefully acknowledge Drs. Sandrine Ding and Sébastien Baechler for their assistance in the statistical analysis.

Conflict of interest The authors declare that they have no conflict of interest.

References

1. Bading JR, Shields AF (2008) Imaging of cell proliferation: status and prospects. J Nucl Med 49(Suppl 2):64S–80S
2. Sherley JL, Kelly TJ (1988) Regulation of human thymidine kinase during the cell cycle. J Biol Chem 263:8350–8358
3. Been LB, Elsinga PH, de Vries J et al (2006) Positron emission tomography in patients with breast cancer using (18)F-3′-deoxy-3′-fluoro-l-thymidine ((18)F-FLT)—a pilot study. Eur J Surg Oncol 32:39–43
4. Yamamoto Y, Nishiyama Y, Ishikawa S et al (2007) Correlation of 18F-FLT and 18F-FDG uptake on PET with Ki-67 immunohistochemistry in non-small cell lung cancer. Eur J Nucl Med Mol Imaging 34:1610–1616
5. Buck AK, Bommer M, Juweid ME et al (2008) First demonstration of leukemia imaging with the proliferation marker 18F-fluorodeoxythymidine. J Nucl Med 49:1756–1762
6. Vesselle H, Grierson J, Muzi M et al (2002) *In vivo* validation of 3′ deoxy-3′-[(18)F]fluorothymidine ([(18)F]FLT) as a proliferation imaging tracer in humans: correlation of [(18)F]FLT uptake by positron emission tomography with Ki-67 immunohistochemistry and flow cytometry in human lung tumors. Clin Cancer Res 8:3315–3323
7. Kameyama R, Yamamoto Y, Izuishi K et al (2009) Detection of gastric cancer using 18F-FLT PET: comparison with 18F-FDG PET. Eur J Nucl Med Mol Imaging 36:382–388
8. Troost EG, Vogel WV, Merkx MA et al (2007) 18F-FLT PET does not discriminate between reactive and metastatic lymph nodes in primary head and neck cancer patients. J Nucl Med 48:726–735
9. Solit DB, Santos E, Pratilas CA et al (2007) 3′-Deoxy-3′-[18F] fluorothymidine positron emission tomography is a sensitive method for imaging the response of BRAF-dependent tumors to MEK inhibition. Cancer Res 67:11463–11469
10. Everitt S, Hicks RJ, Ball D et al (2009) Imaging cellular proliferation during chemo-radiotherapy: a pilot study of serial (18)F-FLT positron emission tomography/computed tomography imaging for non-small-cell lung cancer. Int J Radiat Oncol Biol Phys 75:1098–1104
11. Chen W, Cloughesy T, Kamdar N et al (2005) Imaging proliferation in brain tumors with 18F-FLT PET: comparison with 18F-FDG. J Nucl Med 46:945–952
12. Kenny L, Coombes RC, Vigushin DM, Al-Nahhas A, Shousha S, Aboagye EO (2007) Imaging early changes in proliferation at 1 week post chemotherapy: a pilot study in breast cancer patients with 3′-deoxy-3′-[18F]fluorothymidine positron emission tomography. Eur J Nucl Med Mol Imaging 34:1339–1347
13. Herrmann K, Wieder HA, Buck AK et al (2007) Early response assessment using 3′-deoxy-3′-[18F]fluorothymidine-positron emission tomography in high-grade non-Hodgkin's lymphoma. Clin Cancer Res 13:3552–3558
14. Kostakoglu L, Agress H Jr, Goldsmith SJ (2003) Clinical role of FDG PET in evaluation of cancer patients. Radiographics 23:315–340, quiz 533
15. Higashi K, Clavo AC, Wahl RL (1993) Does FDG uptake measure proliferative activity of human cancer cells? *In vitro* comparison with DNA flow cytometry and tritiated thymidine uptake. J Nucl Med 34:414–419
16. Juweid ME, Cheson BD (2006) Positron-emission tomography and assessment of cancer therapy. N Engl J Med 354:496–507
17. Tian J, Yang X, Yu L et al (2008) A multicenter clinical trial on the diagnostic value of dual-tracer PET/CT in pulmonary lesions using 3′-deoxy-3′-18F-fluorothymidine and 18F-FDG. J Nucl Med 49:186–194
18. Serlin O, Wolkoff JS, Amadeo JM, Keehn RJ (1969) Use of 5-fluorodeoxyuridine (FUDR) as an adjuvant to the surgical management of carcinoma of the stomach. Cancer 24:223–228
19. Kim DW, Ahn DS, Oh YH et al (2006) A new class of SN2 reactions catalyzed by protic solvents: facile fluorination for isotopic labeling of diagnostic molecules. J Am Chem Soc 128:16394–16397
20. Foulon CF, Adelstein SJ, Kassis AI (1996) Kit formulation for the preparation of radiolabeled iododeoxyuridine by demetallation. J Nucl Med 37:1S–3S
21. Dupertuis YM, Vazquez M, Mach JP et al (2001) Fluorodeoxyuridine improves imaging of human glioblastoma xenografts with radiolabeled iododeoxyuridine. Cancer Res 61:7971–7977
22. Marques JP, Maddage R, Mlynarik V, Gruetter R (2009) On the origin of the MR image phase contrast: an *in vivo* MR microscopy study of the rat brain at 14.1 T. Neuroimage 46:345–352
23. Yamamoto Y, Nishiyama Y, Ishikawa S et al (2008) 3′-Deoxy-3′-18F-fluorothymidine as a proliferation imaging tracer for diagnosis of lung tumors: comparison with 2-deoxy-2-18f-fluoro-D-glucose. J Comput Assist Tomogr 32:432–437
24. Barwick T, Benchérif B, Mountz JM, Avril N (2009) Molecular PET and PET/CT imaging of tumour cell proliferation using F-18 fluoro-L-thymidine: a comprehensive evaluation. Nucl Med Commun 30:908–917
25. Direcks WG, Berndsen SC, Proost N et al (2008) [18F]FDG and [18F] FLT uptake in human breast cancer cells in relation to the effects of chemotherapy: an *in vitro* study. Br J Cancer 99:481–487
26. Dupertuis YM, Xiao WH, De Tribolet N et al (2002) Unlabelled iododeoxyuridine increases the rate of uptake of [125I]iododeoxyuridine in human xenografted glioblastomas. Eur J Nucl Med Mol Imaging 29:499–505
27. Dittmann H, Dohmen BM, Kehlbach R et al (2002) Early changes in [18F]FLT uptake after chemotherapy: an experimental study. Eur J Nucl Med Mol Imaging 29:1462–1469
28. Leichman L, Silberman H, Leichman CG et al (1992) Preoperative systemic chemotherapy followed by adjuvant postoperative intraperitoneal therapy for gastric cancer: a University of Southern California pilot program. J Clin Oncol 10:1933–1942
29. Sullivan RD, Miller E (1965) The clinical effects of prolonged intravenous infusion of 5-fluoro-2′-deoxyuridine. Cancer Res 25:1025–1033